ISSN 1068-3356, Bulletin of the Lebedev Physics Institute, 2022, Vol. 49, No. 3, pp. 67–73. © Allerton Press, Inc., 2022.
Russian Text © The Author(s), 2022, published in Kratkie Soobshcheniya po Fizike, 2022, Vol. 49, No. 3, pp. 3–12.

Three Non-Steady-State Photo-EMF Excitation Modes in a Gallium Oxide Crystal

M. A. Bryushinin[a], I. A. Sokolov[a,*], I. N. Zavestovskaya[b,c], R. V. Romashko[d,e], and Yu. N. Kulchin[c,d,e]

[a] *Ioffe Institute, Russian Academy of Sciences, St. Petersburg, 194021 Russia*

[b] *Lebedev Physical Institute, Russian Academy of Sciences, Moscow, 119991 Russia*

[c] *National Research Nuclear University MEPhI, Moscow, 115409 Russia*

[d] *Institute of Automation and Control Processes, Far Eastern Branch of the Russian Academy of Sciences, Vladivostok, 690041 Russia*

[e] *Far Eastern Federal University, Vladivostok, 690922 Russia*

** e-mail: i.a.sokolov@mail.ioffe.ru*

Received December 9, 2021; revised December 9, 2021; accepted January 24, 2022

Abstract—This paper presents the results of measurements of the non-steady-state photo-emf in a monoclinic Ga_2O_3 crystal at a laser wavelength of 457 nm. The crystal has insulating properties and shows high transparency for visible light, which does not prevent the formation of the dynamic space-charge grating and non-steady-state photo-emf signal recording in external (null, dc, and ac) electric fields. The measured signal amplitude is analyzed as a function of the phase modulation frequency, spatial frequency of the interference pattern, and the electric field. The crystal photoconductivity, spectral sensitivity, and diffusion length of photoexcited carriers are determined for the chosen wavelength.

Keywords: non-steady-state photo-emf, adaptive photodetector

DOI: 10.3103/S1068335622030022

1. INTRODUCTION

Monoclinic gallium oxide β-Ga_2O_3 features a unique combination of physicochemical parameters, which provides its applications in various fields of modern electronics and optics. Monoclinic gallium oxide β-Ga_2O_3 with a band gap of ~4.8 eV is transparent in the range from visible to near ultraviolet light; this feature is implemented in solar-blind photodetectors. The material under study is characterized by a strong breakdown field (6–8 MV/cm), a moderate electron mobility, and good thermal stability, i.e., the properties demanded for developing radio-frequency and power field-effect transistors and Schottky diodes. Noteworthy are the proposed techniques for splitting water upon exposure to UV radiation and detecting gases using gallium oxide [1, 2].

The study of Ga_2O_3 photodetectors is as a rule restricted to measurements of the current—voltage characteristic and material response to amplitude-modulated light [3, 4]. There are known techniques based on dynamic holography principles, which make it possible to significantly complement similar studies and improve material diagnostics [5]. The non-steady-state photo-emf effect is one of promising versions for determining the photoelectric parameters of wide band-gap semiconductors [6, 7]. The electric current in a photosensitive medium results from periodic spatial displacements of photoconductivity gratings and space charge with respect to each other. Measurements of the dependence of the signal on the phase modulation frequency and spatial frequency of the interference pattern makes it possible to determine the photoconductivity, carrier lifetimes, mobility and diffusion length, as well as the trap center concentration. This effect is widely used in developing adaptive photodetectors of phase-modulated optical signals [6, 7].

In our recent works, the β-Ga_2O_3 crystal was studied by this method in the green spectral region [8], the diffusion mode of signal excitation was also implemented at wavelength $\lambda = 457$ nm [9]. In this paper, we present the results of the study of the non-steady-state photo-emf effect for three basic signal excitation modes: without an external electric field, as well as in dc and ac fields. The study and comparison of these

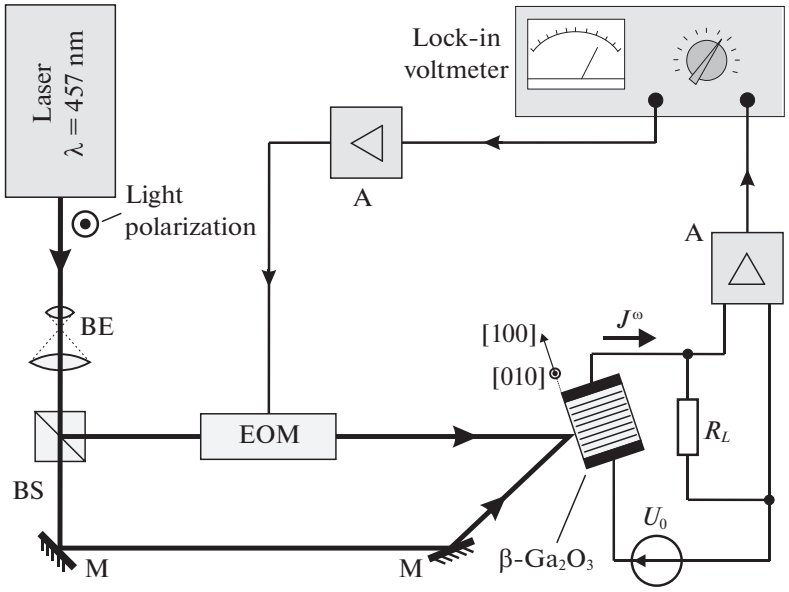

Fig. 1. Experimental setup for studying the non-steady-state photo-emf in an external electric field. BE is the beam expander, BS is the beam splitter, EOM is the electro-optic modulator, M is the mirror, and A is the amplifier.

excitation modes is particularly urgent, since local and nonlocal responses of a material are implemented in them.

2. EXPERIMENTAL SETUP

The experimental setup for studying the non-steady-state photo-emf in β-Ga_2O_3 is shown in Fig. 1. Radiation of the single-frequency solid-state laser with wavelength $\lambda = 457$ nm is expanded and split into two beams. These beams are directed to the crystal where they create an interference pattern with spatial frequency K, contrast m, and average intensity I_0. The signal beam is phase-modulated with amplitude $\Delta = 0.51$ and frequency ω by an electro-optic modulator. The polarization plane of both beams is perpendicular to the incidence plane. The arising photocurrent induces a voltage on a load resistor R_L. This voltage is amplified and then is measured using a selective voltmeter. An external high voltage is supplied by a dc voltage source or a generator with an attached high-frequency transformer.

The frequency of the external sinusoidal voltage is 101 kHz. Before the preamplifier, an additional rejector filter for this frequency is installed to avoid input circuit overload. In experiments with external fields, the following parameters are set: $m = 0.38$, $R_L = 100$ kΩ for zero field, $m = 0.20$, $R_L = 10$ kΩ for a dc field, and $m = 0.38$, $R_L = 5.2$ kΩ for an ac field.

The same β-Ga_2O_3 sample as in our previous studies [8, 9] is studied.

Its sizes are 2.00 × 2.15 × 1.35 mm along crystallographic [100], [010] axes, and the direction perpendicular to the (001) plane, respectively. Front and rear surfaces (2.00 × 2.15 mm) represent cleaved (001) crystal facets; additional treatment was not used.

The current is excited along the [100] ($\mathbf{K} \parallel [100]$) axis; electrodes are deposited on side surfaces perpendicular to this direction.

3. RESULTS AND DISCUSSION

The main thing to be noted is the possibility of reliable detection of the non-steady-state photo-emf signal in the β-Ga_2O_3 crystal excited at a wavelength of 457 nm. The signal has a comparatively small amplitude; nevertheless, reliable detection is reached at a signal-to-noise ratio of 0–40 dB in all three modes considered below.

The signal phase points to the n-type type photoconductivity of a material.

In the absence of an external field, the diffusion excitation mechanism of the non-steady-state photo-emf signal is implemented; the electric field grating arises in the photosensitive medium volume due

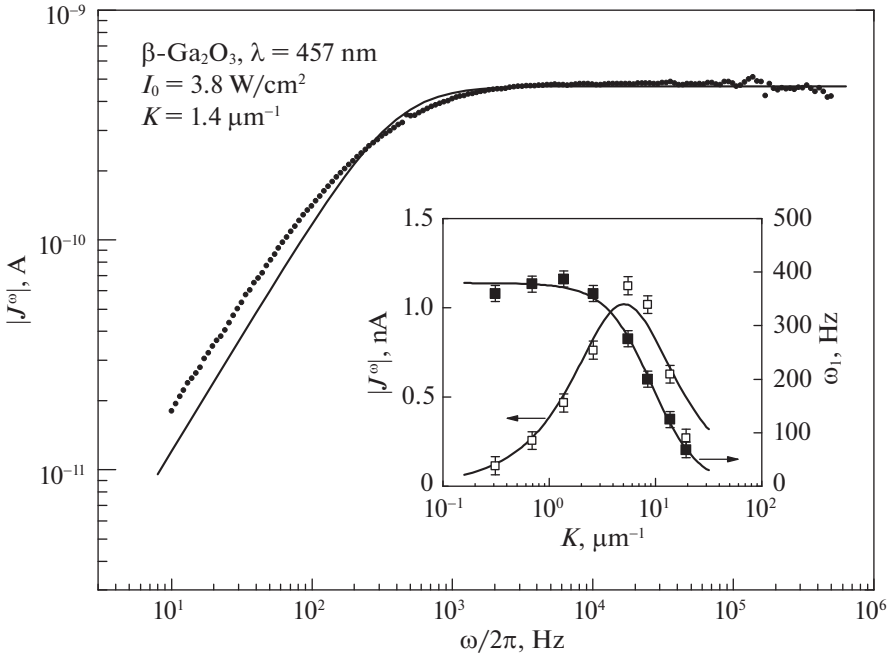

Fig. 2. Frequency dependence of the non-steady-state photo-emf in the diffusion mode of signal excitation ($E_0 = 0$). The inset shows the dependences of the maximum signal amplitude and cutoff frequency on the spatial frequency.

to free carrier diffusion. The frequency dependence of the signal amplitude is shown in Fig. 2. The presented dependence exhibits an increasing portion at low frequencies, followed by a plateau. Such behavior is usually explained as follows: the free electron grating (photoconductivity grating) and space charge field grating trace slow motions of the interference pattern at low excitation frequencies ω.

The relative spatial shift between these gratings is retained to be ~π/2, which yields an insignificant averaged drift current. As ω increases, the space charge grating ceases to trace the pattern shift, becoming almost immobile, relative shifts between gratings increase, and the signal reaches a maximum in the frequency-independent portion. The following expression is known from the effect theory [6, 7] and well describes this behavior,

$$J^{\omega} = S\frac{m^2\Delta}{2}\sigma_0 E_{\mathrm{D}}\frac{-i\omega\tau_{\mathrm{M}}}{1+i\omega\tau_{\mathrm{M}}(1+K^2L_{\mathrm{D}}^2)}, \quad (1)$$

where σ_0 is the average photoconductivity, $E_{\mathrm{D}} = (k_{\mathrm{B}}T/e)K$ is the diffusion field, $\tau_{\mathrm{M}} = \varepsilon_0\varepsilon/\sigma_0$ is the Maxwell relaxation time, L_{D} is the electron diffusion length [5], and S is the electrode area. The cutoff frequency ω_1 divides the signal rise and plateau regions,

$$\omega_1 = [\tau_{\mathrm{M}}(1+K^2L_{\mathrm{D}}^2)]. \quad (2)$$

Measuring the cutoff frequency ω_1, it is easy to estimate the Maxwell relaxation time and sample conductivity (see expression (2) for small K). For chosen intensity $I_0 = 3.8$ W/cm^2, the photoconductivity is $\sigma_0 = 2.3 \times 10^{-9}\ \Omega^{-1}\ \mathrm{cm}^{-1}$. Both the signal amplitude in the region $\omega > \omega_1$ and the cutoff frequency linearly depend on the light intensity, $\left|J^{\omega}\right|, \omega_1 \propto I_0$.

Varying the angle between incident beams, we can vary the spatial frequency K; the corresponding dependence of the signal amplitude is shown in the inset of Fig. 2. The signal increases at small K because of a corresponding increase in the electric field grating amplitude, $J^{\omega} \propto E_{SC} \propto E_{\mathrm{D}} \propto K$. A decrease in the signal at high spatial frequencies K is associated with diffusive "spreading" of the photoconductivity grating. The dependence has a maximum at $K = L_{\mathrm{D}}^{-1}$, and this feature of the non-steady-state photo-emf effect is often used to determine the carrier diffusion length. For the crystal under study, this parameter is $L_{\mathrm{D}} = 200$ nm. The cutoff frequency ω_1 also depends on K (see the inset of Fig. 2 and expression (2)).

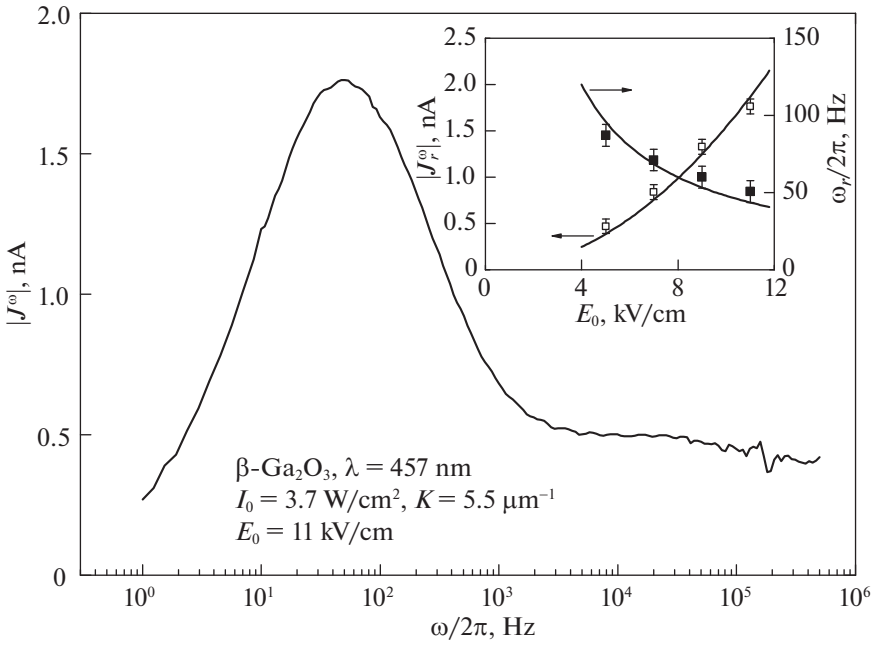

Fig. 3. Frequency dependence of the non-steady-state photo-emf excited in a dc electric field. The inset shows the dependences of the resonant amplitude and resonant frequency on the dc field strength.

This dependence yields a smaller estimate of the diffusion length L_D = 110 nm, which can be attributed to the nonuniform average light intensity.

The non-steady-state photo-emf amplitude can be increased by applying an external dc voltage to the crystal [6, 7]. An increase in the amplitude is not the only change observed in the external field: the frequency dependence of the non-steady-state photo-emf becomes resonant (Fig. 3). This resonant maximum is associated with excitation of the spatial trap recharging wave, i.e., the space charge oscillatory eigenmode in semiconductors [5].

Spatial trap recharging waves propagate along an applied electric field and exhibit an extraordinary dispersion relation, i.e., the dependence $\omega_r(K)$,

$$\omega_r = (\tau_M K L_0)^{-1}. \quad (3)$$

Here $L_0 = \mu\tau E_0$ is the electron drift length in electric field E_0, μ and τ are the electron mobility and lifetime. Such a dispersion relation is indeed observed in our experiments with β-Ga_2O_3.

The spatial trap recharging wave is excited under rather strong electric fields, in which the condition $KL_0 \gg 1 + K^2 L_D^2$ is satisfied. In this case, the non-steady-state photo-emf amplitude reaches

$$J^\omega = S\frac{m^2\Delta}{2}\sigma_0 E_0 \frac{KL_0}{1 + K^2 L_D^2}, \quad (4)$$

exhibiting a quadratic increase in the signal in the dependence on the applied field strength [6].

We measured the dependences of the resonant amplitude and resonant frequency on the dc field E_0 (Fig. 3, inset); their behavior is well consistent with Eqs. (3) and (4).

We note that the resonant maximum appeared much wider than its theoretical evaluation [6]: the width $\delta\omega/2\pi$ = 250 Hz was determined from the experimental dependence of Fig. 3; the width $\delta\omega/2\pi = 2(\omega_r/2\pi)(1 + K^2 L_D^2)/KL_0$ = 23 Hz was calculated for $\omega_r/2\pi$ = 49 Hz and L_D = 200 nm ($\mu\tau = 1.6\times10^{-8}$ cm^2/V). This disagreement is probably associated with the light intensity I_0 and electric field E_0 nonuniformity, as well as with an insufficiently low contrast m which is taken as $m \ll 1$ in the theory.

Applying an external ac voltage is one more method for increasing the non-steady-state photo-emf amplitude. In contrast to the case with an applied dc voltage, the frequency dependence of the signal does not contain resonant features (Fig. 4). The increase in the non-steady-state photo-emf is associated with

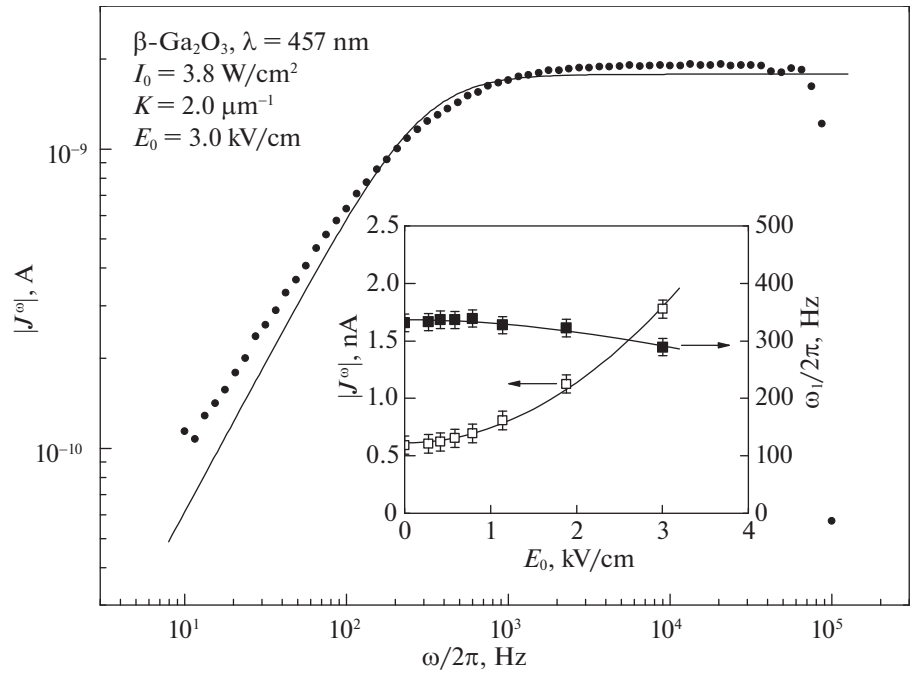

Fig. 4. Frequency dependence of the non-steady-state photo-emf excited in an ac electric field. The inset shows the dependences of the maximum amplitude and cutoff frequency on the effective applied ac field.

the more efficient carrier redistribution between bright and dark interference fringes, which leads to a higher amplitude of the recorded space charge field grating [5]. The increase in the amplitude is accompanied by a decrease in the cutoff frequency; however, the frequency dependence retains the shape characteristic of the diffusion mode of signal excitation [7],

$$J^{\omega} = S\frac{m^2\Delta}{2}\sigma_0 E_{\mathrm{D}}\frac{-i\omega\tau_{\mathrm{M}}(1+E_0^2/E_{\mathrm{L}}^2)}{1+i\omega\tau_{\mathrm{M}}(1+E_0^2/E_{\mathrm{M}}^2)}, \tag{5}$$

$$\omega_{\mathrm{I}} = [\tau_{\mathrm{M}}(1+E_0^2/E_{\mathrm{M}}^2)]^{-1}. \tag{6}$$

Here E_0 is the effective external sinusoidal electric field and $E_{\mathrm{L}} = k_{\mathrm{B}}T/eL_{\mathrm{D}}$ and $E_{\mathrm{M}} = (K\mu\tau)^{-1}$ are characteristic values of this field.

The dependences of the maximum non-steady-state photo-emf amplitude (for $\omega > \omega_{\mathrm{I}}$) and cutoff frequency on the effective applied ac field are shown in the inset of Fig. 4. Approximation of the experimental dependence by expressions (5) and (6) yields one more estimate of the diffusion length, $L_{\mathrm{D}} = 120$–130 nm.

The obtained parameters of the β-Ga_2O_3 crystal are comparable with characteristics of other materials studied in the same spectral region. Since the present and previous experiments were performed under different conditions, i.e., under different light intensities, spatial frequencies, and phase modulation frequencies, we should estimate the normalized maximum photovoltage amplitude,

$$R_m^{\omega} = J_m^{\omega}/[P_0 m^2\, \mathrm{J}_0(\Delta)\,\mathrm{J}_1(\Delta)/2], \tag{7}$$

where J_m^{ω} is the non-steady-state photo-emf amplitude measured at optimum frequencies ($\omega > \omega_{\mathrm{I}}$ and $KL_{\mathrm{D}} = 1$), $P_0 = P_s + P_r$ is the total light power, P_s and P_r are the powers of the signal and reference beams exposing the crystal, $\mathrm{J}_n(\Delta)$ is the n-th-order Bessel function of the first kind. The normalized amplitude is of particular interest in the area of applied interferometry where the contrast and phase-modulation amplitude are commonly small (m, $\Delta \ll 1$). In this case, expression (7) is reduced to $R_m^{\omega} \simeq J_m^{\omega}/(P_s\Delta)$, demonstrating the obvious analogy with the spectral sensitivity of the photodiode [6]. After substituting the values of Fig. 2, we obtain $R_m^{\omega} = 3.8\times10^{-7}$ A/W. This value is lower than that of other wide band-gap materials studied in the blue spectral region, $R_m^{\omega} = 1.1\times10^{-4}$ A/W for $Bi_{12}SiO_{20}$ and $R_m^{\omega} = 3.3\times10^{-5}$ A/W

for SnS_2 [7, 9]. The significant difference in spectral sensitivities is mainly caused by the corresponding difference in light absorbances in these crystals. The small diffusion length L_D (product $\mu\tau$) also leads to a poor sensitivity of β-Ga_2O_3.

Being introduced by expression (7), the spectral sensitivity can also be calculated for modes using the external electric field $R_m^\omega = 2.4\times10^{-6}$ A/W for dc field E_0 = 11 kV/cm and $R_m^\omega = 7.3\times10^{-7}$ A/W for effective ac field E_0 =3.0 kV/cm. Applying an electric field to the β-Ga_2O_3 crystal increases the photovoltage amplitude and spectral sensitivity by several times, rather than by several orders of magnitude as in $Bi_{12}SiO_{20}$ [6, 7]. The cause is the mentioned small product $\mu\tau$ in studied β-Ga_2O_3.

The spectral sensitivity of a material is understood as the phase-modulated light-to-electric current conversion efficiency, rather as the characteristic describing the photodetector capacity to receive weak signals [6]. In the latter case, the noise level should be considered. Since adaptive photodetectors based on the non-steady-state photo-emf usually operate in the short-circuit mode and without external voltages, the noise level is mostly controlled by the thermal noise of the load resistor R_L. In this case, the minimum detected phase-modulation amplitude is defined as $\Delta_{min} = (4k_BTR_L^{-1}\delta f)^{1/2}/(R_m^\omega P_s)$, where δf is the detection band. For the above sensor implementation using the β-Ga_2O_3 crystal, characteristic values P_s = 1 mW and δf = 1 Hz, this amplitude is $\Delta_{min} = 1.1\times10^{-3}$.

Despite the comparatively low sensitivity, certain advantages of β-Ga_2O_3 over other semiconductors can be noted. The non-steady-state photo-emf in the crystal under study features a uniform frequency characteristic in the range of 0.1—500 kHz, whereas the similar dependence in $Bi_{12}SiO_{20}$ decreases at $\omega/2\pi > 3$ kHz. The crystal does not exhibit features associated with shallow traps. The static permittivity of a material is $\varepsilon \approx 10$ [1, 2], while the mentioned sillenite crystal is $\varepsilon = 56$ [5]. This makes it possible to achieve an acceptable cutoff frequency at a lower light intensity.

4. CONCLUSIONS

Photoelectric properties of the β-Ga_2O_3 crystal were studied using the non-steady-state photo-emf method for λ = 457 nm. Photovoltage excitation without any applied voltage and signal amplification under a dc or ac electric field are implemented. The photoconductivity and electron diffusion length were determined for the chosen crystal orientation (**K** $\parallel$ [100]). The acceptable signal level and the frequency characteristic uniformity of the non-steady-state photo-emf in β-Ga_2O_3 are advantages which can be of critical importance in fabricating adaptive photodetectors operating in the short-wavelength visible light spectral region.

FUNDING

The study was supported by the Russian Science Foundation (project no. 19-12-00323).

CONFLICT OF INTEREST

The authors declare that they have no conflicts of interest.

REFERENCES

1. Pearton, S.J., Yang, J., Cary IV, P.H., Ren, F., Kim, J., Tadjer, M.J., and Mastro, M.A., A review of Ga_2O_3 materials, processing, and devices, *Appl. Phys. Rev.*, 2018, vol. 5, p. 011301. https://doi.org/10.1063/1.5006941
2. Stepanov, S.I., Nikolaev, V.I., Bougrov, V.E., and Romanov, A.E., Gallium OXIDE: Properties and applications – a review, *Rev. Adv. Mater. Sci.*, 2016, vol. 44, pp. 63–86.
3. Feng, P., Zhang, J.Y., Li, Q.H., and Wang, T.H., Individual β-Ga_2O_3 nanowires as solar-blind photodetectors, *Appl. Phys. Lett.*, 2006, vol. 88, p. 153107. https://doi.org/10.1063/1.2193463
4. Oshima, T., Okuno, T., Arai, N., Suzuki, N., Ohira, S., and Fujita, S., Vertical solar-blind deep-ultraviolet Schottky photodetectors based on β-Ga_2O_3 substrates, *Appl. Phys. Express*, 2008, vol. 1, no. 1, p. 011202. https://doi.org/10.1143/APEX.1.011202

5. Petrov, M.P., Stepanov, S.I., and Khomenko, A.V., *Photorefractive Crystals in Coherent Optical Systems*, Springer Series in Optical Sciences, vol. 59, Berlin: Springer, 1991. https://doi.org/10.1007/978-3-540-47056-4
6. Stepanov, S., Photo-electromotive-force effect in semiconductors, *Handbook of Advanced Electronic and Photonic Materials and Devices*, Academic Press, 2001, vol. 2, pp. 205–272. https://doi.org/10.1016/B978-012513745-4/50026-3
7. Sokolov, I.A. and Bryushinin, M.A., *Optically Induced Space-Charge Gratings in Wide-Bandgap Semiconductors: Techniques and Applications*, Nova Science, 2017, pp. 1–229.
8. Bryushinin, M.A., Sokolov, I.A., Pisarev, R.V., and Balbashov, A.M., Space-and-time current spectroscopy of a β-Ga_2O_3 crystal, *Opt. Express*, 2015, vol. 23, no. 25, p. 32736. https://doi.org/10.1364/OE.23.032736
9. Bryushinin, M.A., Kulikov, V.V., Petrov, A.A., Sokolov, I.A., Romashko, R.V., and Kulchin, Y.N., Non-steady-state photo-EMF in β-Ga2O3 crystals at $\lambda = 457$ nm, *Opt. Express*, 2020, vol. 28, no. 26, p. 39067. https://doi.org/10.1364/OE.413482

Translated by A. Kazantsev